

RESEARCH ARTICLE

Reaction monitoring via benchtop nuclear magnetic resonance spectroscopy: A practical comparison of *on-line* stopped-flow and continuous-flow sampling methods

Tristan Maschmeyer^{1,2}  | David J. Russell² | José G. Napolitano²  | Jason E. Hein^{1,3,4} 

¹Department of Chemistry, The University of British Columbia, Vancouver, Canada

²Small Molecule Pharmaceutical Sciences, Genentech Inc., South San Francisco, California, USA

³Acceleration Consortium, University of Toronto, Toronto, Canada

⁴Department of Chemistry, University of Bergen, Bergen, Norway

Correspondence

Jason E. Hein, Department of Chemistry, The University of British Columbia, Vancouver, BC V6T 1Z1, Canada.
Email: jhein@chem.ubc.ca

José G. Napolitano, Small Molecule Pharmaceutical Sciences, Genentech Inc., South San Francisco, CA 94080, USA.
Email: napolitano-farina.jose@gene.com

Funding information

Genentech Inc.; The University of British Columbia; Canada Foundation for Innovation (CFI), Grant/Award Number: CFI-35883; Natural Sciences and Engineering Research Council of Canada (NSERC), Grant/Award Numbers: RGPAS-2021-00016, RGPIN-2021-03168

Abstract

The ability for nuclear magnetic resonance (NMR) spectroscopy to provide quantitative, structurally rich information makes this spectroscopic technique an attractive reaction monitoring tool. The practicality of NMR for this type of analysis has only increased in the recent years with the influx of commercially available benchtop NMR instruments and compatible flow systems. In this study, we aim to compare ¹⁹F NMR reaction profiles acquired under both *on-line* continuous-flow and stopped-flow sampling methods, with modern benchtop NMR instrumentation, and two reaction systems: a homogeneous imination reaction and a biphasic activation of a carboxylic acid to acyl fluoride. Reaction trends with higher data density can be acquired with *on-line* continuous-flow analyses, and this work highlights that representative reaction trends can be acquired without any correction when monitoring resonances with a shorter spin–lattice relaxation time (T_1), and with the used flow conditions. *On-line* stopped-flow analyses resulted in representative reaction trends in all cases, including the monitoring of resonances with a long T_1 , without the need of any correction factors. The benefit of easier data analysis, however, comes with the cost of time, as the fresh reaction solution must be flowed into the NMR system, halted, and time must be provided for spins to become polarized in the instrument's external magnetic field prior to spectral measurement. Results for one of the reactions were additionally compared with the use of a high-field NMR.

KEYWORDS

benchtop NMR, *on-line* stopped-flow NMR, *on-line* continuous-flow NMR, process analytical technology, reaction monitoring

This is an open access article under the terms of the [Creative Commons Attribution-NonCommercial](https://creativecommons.org/licenses/by-nc/4.0/) License, which permits use, distribution and reproduction in any medium, provided the original work is properly cited and is not used for commercial purposes.

© 2023 The Authors. *Magnetic Resonance in Chemistry* published by John Wiley & Sons Ltd.

1 | INTRODUCTION

Nuclear magnetic resonance (NMR) spectroscopy is a well-known analytical technique with the ability to provide structurally rich information in a non-destructive and in an inherently quantitative manner.¹ These features are highly valuable assets for reaction monitoring in the pharmaceutical industry, as knowledge of consumption and/or formation of chemical species can help inform critical decisions related to a chemical process. While NMR is generally associated with physically large and expensive superconducting high-field systems, benchtop NMR instruments are providing a viable alternative for certain applications.

Benchtop NMR spectrometers are significantly smaller and cheaper to purchase and maintain. The smaller physical footprint of these systems allow for the structural insights associated with NMR to enter the synthetic laboratory.^{2,3} This is not without tradeoffs, however, as the application of smaller external applied magnetic field strength results in an overall decrease in sensitivity and signal dispersion.⁴

While benchtop NMR may not be a viable option for complex structure elucidation problems due to the limitations highlighted above, reaction monitoring generally entails tracking key resonances, so the impact of these limitations can be minimized. To address the decrease in sensitivity, hyperpolarization techniques^{5,6} may be employed or one can simply monitor a more concentrated reaction solution.^{7,8} In order to decrease the likelihood of resonance overlap, and enhance signal dispersion, one can monitor a nucleus with a large chemical shift range (such as ¹⁹F or ³¹P).^{9,10} If greater signal dispersion cannot be achieved, non-traditional data processing methods, such as Complete Reduction to Amplitude Frequency Table (CRAFT),^{11,12} may be leveraged.

It should be noted that, while benchtop NMR allows for NMR data to be conveniently acquired in a synthetic laboratory, the sample (i.e., reaction solution in this case) must physically be transported to the instrument for analysis. For a reaction ongoing in batch, this implies three primary options: (i) the reaction can be performed on small-scale in an NMR tube itself; (ii) the reaction can be periodically sampled and aliquot transferred to NMR tube for analysis, or (iii) a flow system can be devised such that a portion of the reaction solution is transferred to the NMR magnet for analysis. In the interest of decreasing the human power needed to perform a reaction monitoring analysis, only (i) and (iii) will further be considered.

In 2016, Foley et al. demonstrated the significant differences that one can observe in the reaction rates when observing processes in an NMR tube versus *on-line*

continuous-flow conditions using high-field NMR.¹³ Differences were particularly evident in heterogeneous systems where stirring allowed for more representative mass transfer under 'regular' synthetic conditions.

Much work has been completed in effort to understand the effect of flow on NMR data acquisition; even at the start of this century, a review was written including relevant work on the subject to that point, and with the application to process monitoring.¹⁴ Investigations, however, have continued to enhance our understanding on the subject. For example, Nordon et al. showcased how a pre-magnetization region can assist in increasing the polarization of spins in continuous-flow analyses,¹⁵ and Dalitz et al. highlighted quantitative reaction monitoring with continuous-flow conditions with consideration of the impacts of flow.¹⁶ Additionally, the impact of flow rate and flow cell geometry on flow behaviour has been studied,¹⁷ and the necessary hardware considerations one must make when designing a flow NMR system (such as choice of pump and resultant pulsation of analyte) has more recently been reported.¹⁸ Recent investigations of *on-line* continuous-flow conditions for NMR measurements with a modern high-field NMR system¹⁹ and a modern benchtop NMR system⁸ have been conducted with application to reaction monitoring in mind.

Recently, the authors have demonstrated the utility of an *on-line* stopped-flow benchtop NMR system where we quantitatively monitored reaction systems.⁹ This *on-line* stopped-flow system is analogous type to a stopped-flow system applied as far back as the 1980s for reaction monitoring²⁰ and different than the *in situ* stopped-flow systems employed for monitoring rapid reactions, where fundamentally those systems are used to minimize the time between initiation of the reaction and data acquisition.^{21–23} This *on-line* stopped-flow system is a closed-loop flow batch system, as solution circulates through the NMR instrument and reactor, but the solution is halted in the magnet just prior and during NMR data collection (Figure 1). After data acquisition, the solution returns to continuous circulation until the next data acquisition event. Using this method, NMR measurements are conducted under static conditions, so irregularities of hardware that can be detrimental to NMR measurements, such as pump pulsation, are a non-issue so long that sufficient time for analyte to stabilize is provided prior to data acquisition.

In this manuscript, reaction profiles are acquired under *on-line* stopped-flow and continuous-flow sampling conditions with a modern, commercially available benchtop NMR instrument and accompanied flow cell. Acquired data and reaction trends are directly compared, with the desire to reduce complexity of data analysis and allow for approachable reaction monitoring analyses for

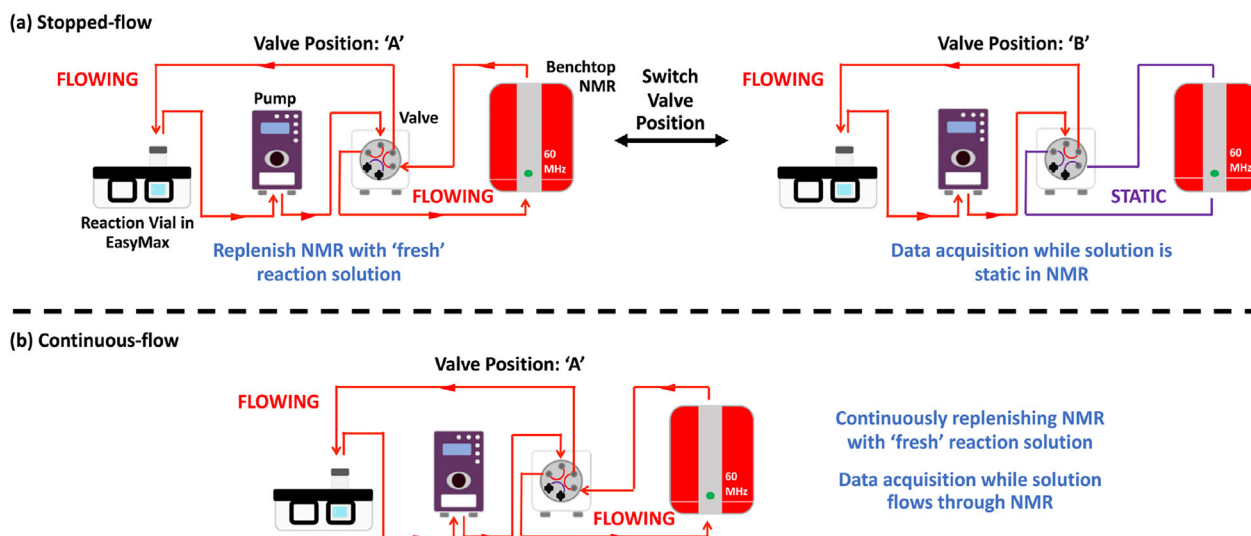


FIGURE 1 Schematic of the NMR flow systems compared in this study for (a) *on-line* stopped-flow analyses and (b) *on-line* continuous-flow analyses.

a non-NMR specialist. This was of particular interest as the extent of flow effects are known to be specific to magnet configurations¹⁹; therefore, these empirical observations may be of interest for users of similar systems. Two reactions were monitored in this effort: a homogeneous imination reaction between 4-fluoroaniline and 4-fluorobenzaldehyde and a biphasic activation reaction of 4-fluorobenzoic acid with perfluorobutanesulfonyl fluoride (PBSF) to the corresponding acyl fluoride. In either case, reactions were additionally performed in a 5 mm NMR tube as a benchmark measurement.

2 | MATERIALS AND METHODS

2.1 | Materials

All materials were obtained from commercial sources and used as received. 4-Fluoroaniline, 4-fluorobenzaldehyde, 4-fluorobenzoic acid, PBSF and diisopropylethylamine (DIPEA) were obtained from Sigma-Aldrich and used as received. Additionally, acetonitrile (MeCN) and methanol (MeOH) were obtained from Fisher Scientific.

2.2 | NMR instrumentation and data acquisition

NMR measurements were conducted on a 1.46 T Magritek Spinsolve 60 benchtop NMR system (^1H : 62 MHz, ^{19}F : 58 MHz) and a 11.74 T Bruker AVANCE III HD

system (^1H : 500 MHz, ^{19}F : 471 MHz) equipped with a nitrogen-cooled Prodigy broadband probe.

Concentration of species were determined by converting absolute NMR integrations to concentrations. This was completed using an external calibration qNMR method where a single concentration conversion factor was applied to all resonances for a given reaction and sampling method. A conversion factor was determined with each sampling method (5 mm NMR tube, stopped-flow, continuous-flow) by comparing the absolute integration of a resonance to the known gravimetric concentration.

2.3 | Benchtop NMR flow system

The benchtop NMR *on-line* stopped-flow system (Figure 1) consisted of three hardware components: a benchtop NMR spectrometer, a peristaltic pump (Vapourtec SF-10 reagent pump) and a six-way valve (Vici C2, two-ports plugged). These components were connected by either ethylene tetrafluoroethylene [ETFE, 1/16" outer diameter (O.D.), 0.02" inner diameter (I.D.)] or polyether ether ketone (PEEK, 1/16" O.D., 0.01" I.D.) tubing. No thermal regulation of these lines was implemented, as a lack of thermal regulation is a known and well-established limitation of many benchtop NMR instruments. With this temperature consideration in mind, all reaction solutions in the primary reaction flask (either NMR tube or scintillation vial) were maintained at 26°C (internal temperature of magnet) to ensure the integrity of direct comparisons between analysis techniques.

In addition to the hardware components listed above, an NMR glass flow cell from the instrument manufacturer was used where the analyte solution entered from the bottom of the instrument and exited the top. The entire volume of this system, with all tubing to/from the reaction flask and the glass flow cell, was determined to be 1.76 mL (Supporting Information Section S2.c).

For *on-line* stopped-flow analyses (Figure 1a), an internally developed Python script was used. This script allowed central control of pump flow rate, valve position and benchtop NMR data acquisition (experiment, acquisition parameters, number of spectra and overall time between spectra).

Reaction solution initially was pumped from the flask through the valve and NMR flow cell, returning to the flask (valve position 'A'). At a pre-determined timepoint, the valve position switched (valve position 'B'), resulting in the reaction solution being pumped from the reaction flask to the valve and returning to the flask, without entering the NMR loop. After a lock and calibrate protocol, and pre-magnetization time in this static condition, data were acquired. Once acquisition completed, the valve position switched (position 'A') to allow for reaction solution to be replenished and the procedure repeats.

For *on-line* continuous-flow analyses (Figure 1b), the same hardware system and Python script were used, but the valve position was not toggled through the reaction course (i.e., valve remained in position 'A'). This allowed for the reaction mixture to continuously flow through the system, with data acquisition occurring as the sample flowed through the spectrometer.

In all flow analyses, a flow rate of 2.7 mL/min was used. This flow rate resulted in a 38 s residence time for analyte within the entire benchtop NMR flow system (valve position 'A') and allowed for a timely transfer of reaction solution from the reaction flask to the benchtop NMR for analysis. It is acknowledged that a slower flow rate may be leveraged and may be beneficial in enhancing polarization in continuous-flow analyses. However, this comes at the expense of lengthening the time to which reaction solution is exposed to conditions not representative of the reaction flask (e.g., if reaction flask is heated/cooled or mechanically stirred).

2.4 | High-field NMR flow system

An *on-line* flow system analogous to that shown in Figure 1b was used to acquire continuous-flow data on a reaction mixture (see Supporting Information Section S2.d) using a high-field NMR system. The only hardware difference occurred in the incorporation of a Bruker

InsightMR flow system along with a high-field NMR spectrometer. Additionally, during reaction monitoring trial, a lock and calibrate protocol was not necessary with the used Bruker spectrometer prior to data acquisition.

2.5 | Procedures for imination reaction

For both stopped- and continuous-flow trials, 1:1 MeCN:MeOH (7.20 mL) was added to septum capped vial equipped with a magnetic stir bar. This solution was then circulated through the flow system at a flow rate of 2.7 mL/min. To this vial 4-fluorobenzaldehyde (0.18 mL, 1.7 mmol, 1.0 eq.) was added, followed by 4-fluoroaniline (0.18 mL, 1.9 mmol, 1.1 eq.). After mixing, the Python script controlling data acquisition was started.

For the reaction completed in a 5 mm NMR tube, 1:1 MeCN:MeOH (1.00 mL) was added to an NMR tube, followed by 4-fluorobenzaldehyde (0.025 mL, 0.23 mmol, 1.0 eq.) and 4-fluoroaniline (0.025 mL, 0.26 mmol, 1.1 eq.). The tube was inverted multiple times to achieve good mixing and was entered into the NMR spectrometer. The Python script was then started (pump and valve not used, lines commented out in code) controlling data collection.

Spectra were collected every 250 s, and a lock and calibration protocol (~ 55 s), followed by 20 s pause time, was completed just before each $^{19}\text{F}\{^1\text{H}\}$ NMR experiment was initiated. For the stopped-flow trial, 25 spectra were acquired, where for continuous-flow and 5 mm NMR tube reaction, 36 spectra were collected in total. Additionally, due to the lock and calibration protocol and designated pause time, ~ 75 s was supplied for the reaction solution to stabilize in the NMR prior to spectral measurement in the case of stopped-flow analysis.

In all cases $^{19}\text{F}\{^1\text{H}\}$ NMR data were collected with a 90° pulse, 1 scan, 0 dummy scans, 1.64 s acquisition time, 5,000 Hz (85.9 ppm) spectral width, -115 ppm spectral offset, and a 4 s repetition time.

2.6 | Procedures for activation of carboxylic acid with PBSF

For both *on-line* stopped- and continuous-flow trials, 4-fluorobenzoic acid (stopped-flow: 349.954 mg, 2.4 mmol, 1 eq.; continuous-flow: 349.928, 2.4 mmol, 1.0 eq.) was weighed into a septum capped vial. To this vial, MeCN (7.20 mL) was added and was equipped with a magnetic stir bar. DIPEA (0.54 mL, 3.0 mmol, 1.2 eq.) was next added. This solution was then circulated through the flow system, with flow rate of 2.7 mL/min. Finally, PBSF (0.54 mL, 2.7 mmol, 1.1 eq.) was added.

After mixing, data acquisition was started and only the MeCN layer was sampled. This was achieved as the PBSF layer was both small ($\sim 6\%$ of the total initial volume) and more dense than the MeCN layer. Therefore, by placing the intake line near the surface of the liquid level, we were able to ensure only the MeCN layer was pumped through the system and sampled with the NMR.

For the reaction completed in a 5 mm NMR tube, 4-fluorobenzoic acid (39.427 mg, 0.28 mmol, 1.0 eq.) was weighed into a vial. To this vial, MeCN (0.80 mL), DIPEA (0.060 mL, 0.34 mmol, 1.2 eq.), and PBSF (0.055 mL, 0.31 mmol, 1.1 eq.) were added. Upon quickly mixing the contents of the vial, the entire solution was transferred to a 5 mm NMR tube and entered into the NMR spectrometer such that only the MeCN soluble layer was within the reading frame of the instrument. The Python script was then started for data collection where the pump and valve were not active.

Spectra were collected every 540 s for the stopped-flow and continuous-flow analyses and every 600 s for the reaction performed in a 5 mm NMR tube. A lock and calibration protocol (~ 55 s), followed by 40 s pause time, was completed just before each $^{19}\text{F}\{^1\text{H}\}$ NMR experiment was initiated. For stopped-flow, continuous-flow, and 5 mm NMR tube reactions, 132, 129, and 394 spectra were collected in total, respectively. Additionally, due to the lock and calibration protocol and designated pause time, ~ 95 s was supplied for the reaction solution to stabilize in the NMR prior to spectral measurement in the case of stopped-flow analysis. Additionally, as the reaction progressed, all reaction solutions became homogeneous.

In all cases (stopped- or continuous-flow, 5 mm NMR tube), $^{19}\text{F}\{^1\text{H}\}$ NMR data were collected with a 90° pulse, 1 scan, 0 dummy scans, 1.64 s acquisition time, 5,000 Hz (85.9 ppm) spectral width, -100 ppm spectral offset, and a 10 s repetition time.

For the high-field continuous-flow/no flow trial, 4-fluorobenzoic acid (459.500 mg, 3.2 mmol, 1 eq) was weighed into a septum capped vial. To this vial, MeCN (9.48 mL) was added and was equipped with a magnetic stir bar. To this solution, DIPEA (0.70 mL, 3.9 mmol, 1.2 eq.) was added. This solution was then circulated through the flow system, with flow rate of 2.7 mL/min. Finally, PBSF (0.70 mL, 3.6 mmol, 1.1 eq.) was added. Only the MeCN layer was sampled.

After manual acquisition of the first ^{19}F NMR spectrum, additional datasets were acquired utilizing the Bruker 'multi_zgvd' command where the 90 spectra were collected with a 613 s fixed delay. For the first 90 minutes, data were acquired under continuous-flow conditions. For the remainder of the trial, data were acquired on the static solution as the pump was turned

off for the remainder of the time. The ^{19}F NMR data were acquired with a 90° pulse, 1 scan, 0 dummy scans, 1.50 s acquisition time, 208,333 Hz (442.7 ppm) spectral width, -100 ppm spectral offset, and a 6.5 s repetition time.

3 | RESULTS AND DISCUSSION

3.1 | Homogeneous imination reaction

The coupling of 4-fluorobenzaldehyde (**1**) and 4-fluoroaniline (**2**) to prepare the corresponding imine (**3**) was performed in batch and monitored by both *on-line* stopped-flow and continuous-flow techniques. Additionally, this reaction was performed and monitored in a 5 mm NMR tube. This system was selected as it represented a homogeneous reaction system similar to the reaction analyzed by Foley et al. in 2016¹³ where trends resulting from the reaction performed in a 5 mm tube (with and without periodic inversion) and under *on-line* continuous-flow conditions were directly compared.

This reaction system (along with activation reaction to follow) was monitored via $^{19}\text{F}\{^1\text{H}\}$ NMR. This was the desired method as there was no solvent signal in the resulting spectra and the greater signal dispersion helped with accurately quantifying resonances without the need of advanced spectral processing and analysis. Furthermore, the ^1H decoupling consolidated each of the aryl fluoride signals to a singlet, resulting in better digitization of resonances and overall reducing the impact of the sensitivity limitation associated with benchtop NMR.

For this reaction and all monitoring techniques (*on-line* stopped-flow, *on-line* continuous-flow, or 5 mm NMR tube), resonances consistent with each species were readily observed. The consumption of **1** and **2** could be monitored with the disappearance of resonances with chemical shifts of δ_{F} -105.0 ppm and -129.6 ppm, respectively. Additionally, the appearance of two fluorine resonances with chemical shifts of δ_{F} -110.0 ppm and -118.9 ppm were consistent with the formation of the desired imine product **3**. Representative data for this transformation for the *on-line* stopped-flow monitoring trial can be found in Figure 2.

The reaction profiles tracking each component, with each analysis method, was directly compared (Figure 3, Supporting Information Section S4). With this homogeneous reaction system, excellent agreement in reaction rates when tracking each of the components with *on-line* stopped-flow and continuous-flow analysis methods was observed. This can be seen both qualitatively in the reaction trends and quantitatively by monitoring the apparent rate constants when fitting the reaction trends to a first-order exponential. Additionally, no difference in

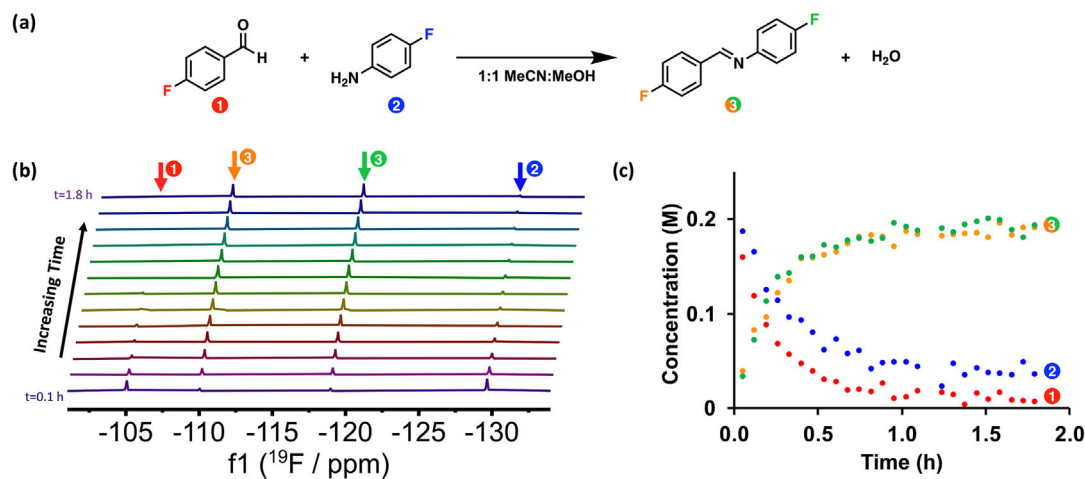


FIGURE 2 (a) Reaction scheme for coupling **1** (0.22 M, 1.0 eq., δ_F –105.0 ppm) and **2** (1.1 eq., δ_F –129.6 ppm) to form corresponding imine **3** (δ_F –110.0 and –118.9 ppm) in 1:1 MeCN:MeOH. (b) Representative decimated stacked array of $^{19}\text{F}\{^1\text{H}\}$ NMR spectra (58 MHz) of the transformation when monitored via *on-line* stopped-flow NMR. (c) Reaction profile resulting from tracking each resonance with time.

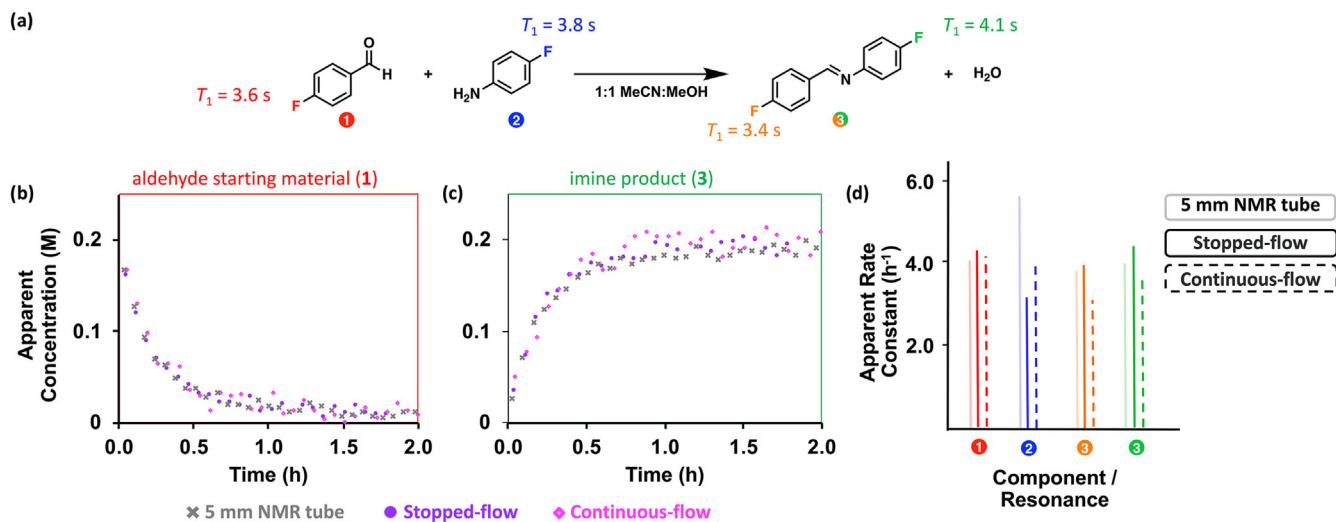


FIGURE 3 (a) Reaction scheme for coupling **1** (0.22 M, δ_F –105.0 ppm) and **2** (1.1 eq., δ_F –129.6 ppm) to form the corresponding imine **3** (δ_F –110.0 and –118.9 ppm), along with estimated T_1 values of each fluorine resonance. Observed reaction trends from $^{19}\text{F}\{^1\text{H}\}$ NMR spectra (58 MHz) for two representative reaction species monitored via *on-line* stopped-flow (purple circle), *on-line* continuous-flow (open pink diamonds) and reaction performed in 5 mm NMR tube (grey cross): (b) aldehyde starting material (**1**) and (c) imine product (**3**). (d) Apparent rate constants for each component/resonance when fitted to first-order exponential.

reaction trends resulted when comparing each of the flow methods (*on-line* stopped- and continuous-flow) and the reaction conducted in a 5 mm NMR tube. Though some deviation existed in the aniline reaction profile and apparent rate constant with a 5 mm NMR tube, likely caused from error in measuring such a small volume. Overall, this suggests that the reaction solution in the 5 mm NMR tube was well mixed and the reaction was not diffusion limited.

It should be mentioned that the spin–lattice relaxation time (T_1) dictates the time needed for adequate polarization of spins prior to application of a

radiofrequency (RF) pulse after the sample is both introduced into an instrument's external applied magnetic field and after the application of RF pulse. This constant can be estimated using methods such as the inversion-recovery sequence^{24,25} or Faster Longitudinal relaxation Investigated by Progression Saturation.²⁶

Further, it should be noted that the T_1 of a nucleus is a physical constant for a particular resonance at a particular external field strength, temperature and concentration. Therefore, depending on residence time of analyte under continuous-flow conditions and the T_1 for a resonance, spins may not become fully polarized prior to

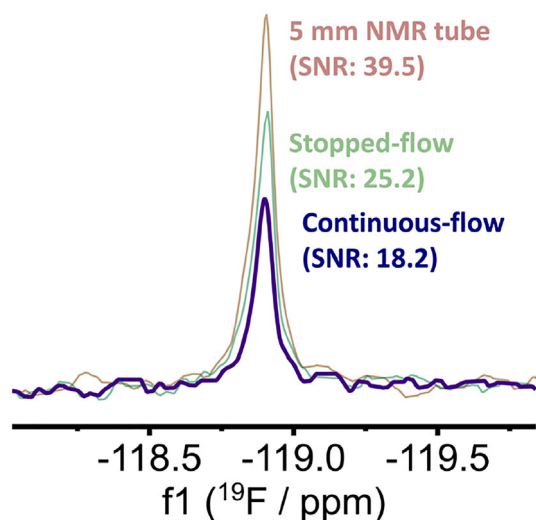


FIGURE 4 Superimposed NMR spectra ($^{19}\text{F}\{^1\text{H}\}$, 58 MHz, normalized to noise) for an imine product **3** resonance ($\delta_{\text{F}} -118.9$ ppm) from the same timepoint of the reaction. Spectra showcase the relative SNR differences for data acquired with the same acquisition parameters between 5 mm NMR tube analysis (orange), *on-line* stopped-flow (green) and *on-line* continuous-flow (blue) analyses.

NMR measurement. This is referred to as ‘in-flow’ effects. Furthermore, a T_1 value estimated under continuous-flow conditions does not represent the true T_1 of the resonance, rather a complex relationship to reach maximum signal polarization considering non-polarized spins entering, polarized spins pulsed and observed, and polarized spins leaving the reading frame. This is referred to as ‘out-flow’ effects.

While these phenomena have been known for decades, the work by Hall et al. has nicely described these effects with a modern high-field NMR instrumentation and highlighted a simple correction factor to compensate for in-flow effects.¹⁹ Additionally, Bara-Estaún et al. recently highlighted the use of paramagnetic relaxation agents in flow NMR analyses, allowing for faster polarization of spins.²⁷

For each component of this imination reaction system, the true T_1 values of each of the aryl fluoride resonances were estimated using the inversion-recovery method under static conditions (Supporting Information Section S3.a). The T_1 values for all ^{19}F resonances were estimated to be similar and ~ 4 s or less (Figure 3a, Supporting Information Section S3.a). While sufficient time for polarization buildup was confidently supplied in our *on-line* stopped-flow and 5 mm NMR tube experiments, the nature of reaction profiles for the continuous-flow analysis suggest that a relatively equal polarization steady-state was additionally achieved prior to $^{19}\text{F}\{^1\text{H}\}$ NMR measurements.

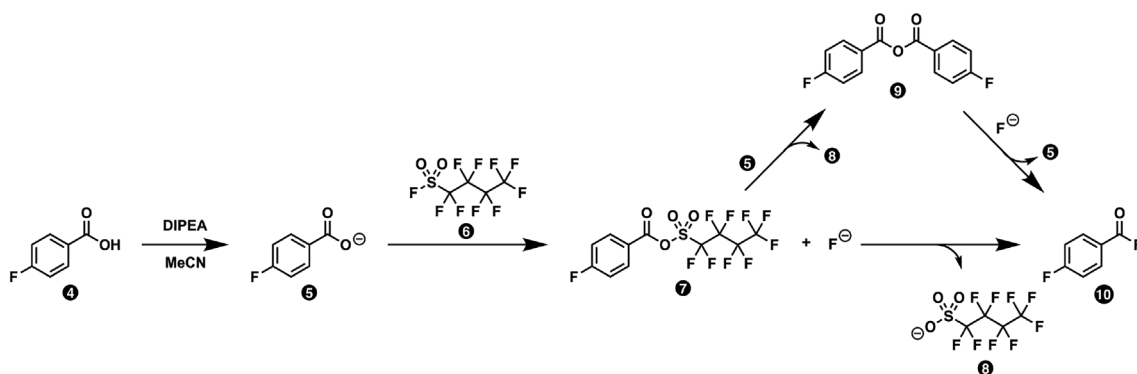
While these imination reaction data highlight the consistent reaction profiles that may be achieved with either *on-line* stopped-flow or continuous-flow monitoring techniques for when all monitored resonances possess reasonable T_1 values, differences arise in the SNR for a given resonance, acquired with the same number of scans with each technique (Figure 4). This highlights a consideration that may alone lead one to choose one monitoring technique over another with a benchtop NMR system.

In the case of *on-line* stopped-flow, the reaction mixture was halted in the active volume of the instrument for well over $5 \times T_1$ prior to pulse excitation. This means that over 99% polarization was achieved, leading to a maximum amount of signal to be acquired considering the analyte within the active volume of the flow cell. Under *on-line* continuous-flow conditions, however, the same amount of analyte is present within the active volume, but the previously described in-flow effects overall decrease the amount of polarization of spins, and therefore signal. As an example, for the imine product resonance at $\delta_{\text{F}} -118.9$ ppm the continuous-flow 0.4 h timepoint showcased 72% of the SNR for the stopped-flow analysis at the same timepoint.

Therefore, it should be highlighted that while more data points per unit time could be acquired with *on-line* continuous-flow analyses, these results suggest that the data density comes at an intrinsic SNR cost when considering data acquired with the same acquisition. Additionally, if a relatively high data density is acquired, consideration of the ‘out-flow’ effects and the time between spectral measurements may be necessary. In contrast, the relative increase in sensitivity for *on-line* stopped-flow analyses, comes at a cost of time as the NMR flow cell must be replenished, the flow must be halted, and time must be supplied for polarization of spins prior to measurement of an NMR spectrum.

Additionally, it is important to note that without the replenishment and polarization steps, more scans per data point could be acquired with *on-line* continuous-flow analyses, therefore increasing sensitivity of these measurements. While possible, it would become imperative to consider the repetition time and the ‘out-flow’ effects on the apparent T_1 values with signal averaged data—where the need for further correction factors may result.²⁸ Therefore, this inherent sensitivity trade-off and/or complexity of data analysis represents important considerations when selecting an appropriate sampling method for a reaction system with resonances with reasonable T_1 values.

When comparing the data from *on-line* stopped-flow and 5 mm NMR tube analyses, in either case sufficient time for polarization of spins was supplied ($>5 \times T_1$).



SCHEME 1 Plausible reaction pathways for the activation of 4-fluorobenzoic acid (**4**) with PBSF (**6**) in the presence of diisopropylethylamine (DIPEA) to access the associated acyl fluoride **10**.

Therefore, the difference in observed SNR can be rationalized purely from the difference in the amount of analyte present in the active volume of the NMR instrument between the 5 mm NMR tube itself and the glass flow cell. The larger internal volume of the 5 mm NMR tube suggests more spins in the active volume that can in turn be excited, resulting in more signal and higher SNR. For one of the imine products resonances ($\delta_{\text{F}} -118.9$ ppm), the stopped-flow 0.4 h timepoint showcased 64% of the SNR than the 5 mm NMR tube analysis at the same timepoint.

Overall, this homogeneous reaction example highlights that while consistent reaction trends may be able to be acquired with either *on-line* stopped- or continuous-flow analyses, there will be an intrinsic SNR benefit considering data measured with the same number of scans. For the case of reaction monitoring, where observation of low-level species (intermediates, side-products *etc.*) is often desired, *on-line* stopped-flow can provide the maximum SNR for a particular flow cell and set of data acquisition set, and without the introduction of correction factors for either ‘in-flow’ or ‘out-flow’ effects. Most importantly, this relative SNR maximum is of interest with the decrease in sensitivity inherent to benchtop NMR systems.

3.2 | Heterogeneous (biphasic) carboxylic activation

PBSF has long been reported as a reagent used in the deoxyfluorination of alcohols.²⁹ Our lab has been involved in a similar transformation,^{9,30} monitoring the activation of a carboxylic acid to the corresponding acyl fluoride with sulfonyl fluoride (SO_2F_2), a toxic gaseous reagent. We therefore sought to perform a similar transformation with a commercially available liquid substitute. The goal was to monitor the activation of

4-fluorobenzoic acid (**4**) with PBSF (**6**) to prepare the corresponding acyl fluoride (**10**). The reaction was studied via $^{19}\text{F}\{^1\text{H}\}$ NMR.

While monitoring this reaction with the various techniques (*on-line* stopped-flow, *on-line* continuous-flow, 5 mm NMR tube), aryl fluoride resonances consistent with the carboxylic acid starting material, an intermediate (later identified as symmetrical intermediate **9**, see Scheme 1 and Supporting Information Section S5.b), and acyl fluoride product were readily observed. The aryl fluoride resonances consistent with these species were observed with chemical shifts of $\delta_{\text{F}} -112.5$, -103.0 , and -101.3 ppm for species **4**, **9** and **10**, respectively. Representative data for this transformation for the stopped-flow monitoring trial can be found in Figure 5.

Similar to the analysis conducted with the previous homogeneous imination reaction, reactions sampled under *on-line* continuous-flow conditions resulted in the lowest SNR, *on-line* stopped-flow with a relatively higher SNR, and the reaction performed in an NMR tube resulted in the highest SNR for a given mole fraction conversion timepoint and data collected with the same acquisition. The reasons for these observed SNR differences are consistent with those as previously described for the imination reaction.

Further, reaction profiles and apparent rate constants for this reaction system, with each analysis method, were directly compared (Figure 6). Considering carboxylic acid starting material **4** of this heterogeneous, biphasic reaction system, reaction trends and apparent rate constants acquired under *on-line* stopped-flow and continuous-flow conditions showcased great agreement. Additionally, consistent with literature,¹³ monitoring this resonance and reaction with flow resulted in a significantly faster reaction compared with if the reaction is performed in a 5 mm NMR tube. This can be observed qualitatively with the reaction trends or quantitatively with the apparent rate constants when fit to first-order exponential. This

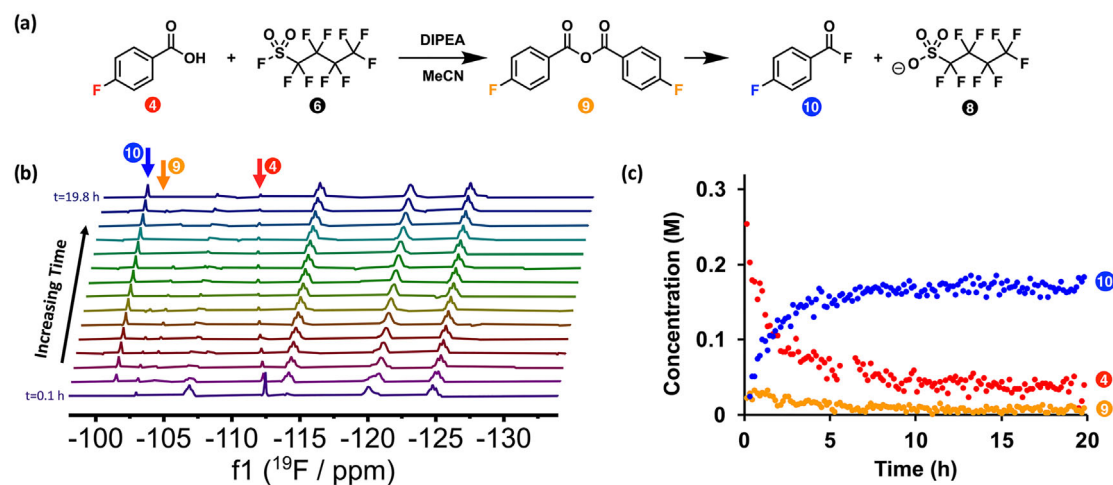


FIGURE 5 (a) Reaction scheme for the activation of **4** (0.30 M, 1.0 eq., $\delta_{\text{F}} -112.5$ ppm) with **6** (1.1 eq.) to form the corresponding acyl fluoride **10** ($\delta_{\text{F}} -101.3$ ppm) in MeCN with DIPEA (1.2 eq.). (b) Representative zoomed decimated stacked array of $^{19}\text{F}\{^1\text{H}\}$ NMR spectra (58 MHz) of the transformation when monitored via *on-line* stopped-flow NMR. (c) Reaction profile resulting from tracking each resonance with time.

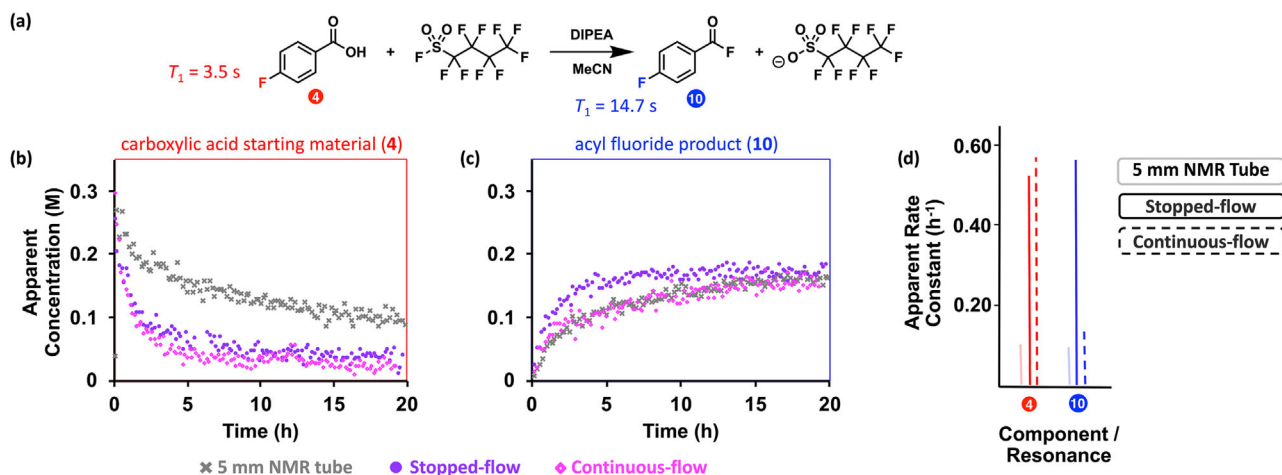


FIGURE 6 (a) Reaction scheme for the activation of **4** (0.30 M, 1.0 eq., $\delta_{\text{F}} -112.5$ ppm) to form the corresponding acyl fluoride **10** ($\delta_{\text{F}} -101.3$ ppm) using PFSF (**6**, 1.1 eq.), along with estimated T_1 values for the two aryl fluoride resonances. Observed reaction trends from $^{19}\text{F}\{^1\text{H}\}$ NMR spectra (58 MHz) are compared for each component monitored via *on-line* stopped-flow (purple circle), *on-line* continuous-flow (open pink diamonds), and reaction performed in 5 mm NMR tube (grey cross): (b) carboxylic acid starting material **4** and (c) aryl fluoride of acyl fluoride product **10**. (d) Apparent rate constants for each component/resonance when fitted to first-order exponential.

expected behaviour is consistent with more efficient mass transfer as a result of stirring in the reaction flask when performed in batch.

Interestingly, when comparing reaction trends for the aryl fluoride resonance of acyl fluoride product **10**, the reaction profiles and apparent rate constants acquired with *on-line* stopped-flow and continuous-flow analyses were not in agreement. Instead, the *on-line* stopped-flow analysis suggested faster product formation, unexpected as the reactions were performed under the same conditions (scale, temperature *etc.*). Furthermore, the reaction performed in a 5 mm NMR tube resulted in a slower

reaction trend than that monitored via stopped-flow as expected, but unexpectedly matched that from the *on-line* continuous-flow trial.

Upon consideration of the resulting reaction trends and estimation of aryl fluoride T_1 values, it was hypothesized that the previously described ‘in-flow’ effect of flow on resonance polarization was an influencing factor in the discrepancy. The estimated T_1 of the aryl fluoride of product **10** (14.7 s) was significantly longer than that of the carboxylic acid starting material (3.5 s). Therefore, we posit the very long T_1 of the product’s aryl fluoride resonance results in inadequate buildup of polarization

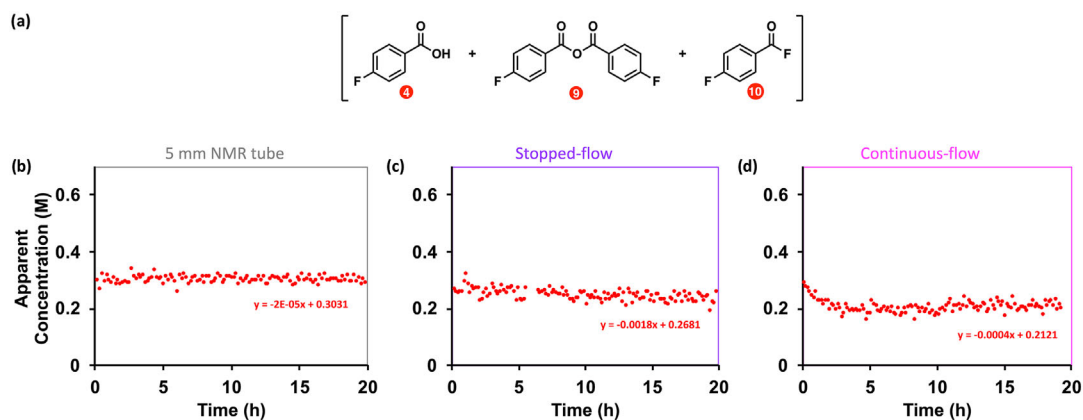


FIGURE 7 (a) Summation of reaction component concentrations used for uncorrected mass balance analysis. (b) Results of uncorrected mass balance with line equation for linear line of best fit displayed (line not shown) for (b) 5 mm NMR tube, (c) *on-line* stopped-flow and (d) *on-line* continuous-flow.

prior to $^{19}\text{F}\{^1\text{H}\}$ spectral acquisition during the *on-line* continuous-flow analysis.

While the use of correction factors has been reported to compensate for such deviations due to ‘in-flow’ effects,¹⁹ this may have been applied for a more accurate representation of the apparent concentration over time for **10** under *on-line* continuous-flow conditions. However, even without correction, the apparent rate constant would be expected to be in agreement with the *on-line* stopped-flow trial, so long that the apparent T_1 and all other physical factors (such as pump flow rate) remain unchanged throughout the reaction.

Therefore, the disagreement between *on-line* stopped-flow and continuous-flow rate constants for **10** suggest some inconsistencies through the course of the reaction. For instance, T_1 values are known to be dependent on many physical properties, such as viscosity of solvent, concentration and temperature.^{31,32} As the species is being formed through the reaction, the concentration inherently changed (from 0 M to ~ 0.2 M). Additionally, as the reaction went from a heterogeneous, biphasic solution, to a homogeneous solution, a change in viscosity of the reaction solvent is evident. Not only could a change in viscosity directly impact the T_1 values directly, but this could further impact the flow rate, intrinsically changing the ‘in-flow’ and ‘out-flow’ effects. Therefore, with the many factors that would need be accounted for to accurately monitor this dynamic system over the entire reaction course, we avoided the application of a correction factor in effort to simplify data analysis, with the ultimate goal of highlighting a method for robust walk-up analyses for our synthetic chemist colleagues.

Additionally, analysis of the apparent mass balance with acquired $^{19}\text{F}\{^1\text{H}\}$ NMR data (Figure 7) from the *on-line* continuous-flow trial is further consistent with our

previous hypothesis of inadequate polarization of the resonance consistent with the aryl fluoride of **10**. While the apparent mass balance is expected to be constant throughout the reaction course if any and all flow effects are accounted for, the sum of aryl fluoride concentrations for continuous-flow monitoring showcased a decrease over the first 5 h, followed by a slow increase over the remainder of time. This is in contrast to the mass balance trends of that from the 5 mm NMR tube and *on-line* stopped-flow trials that showcased a mass balance closer to what would be expected. Therefore, the uncorrected *on-line* continuous-flow data are consistent with the underestimation of a reaction component over the time course as the product is being formed.

While all previous data were acquired on a benchtop NMR instrument, we were curious if the inadequate polarization of acyl fluoride **10** would be observed to the same extent with the utilization of a high-field NMR instrument. The magnitude of the impacts of flow on NMR data have been documented to be dependent on magnet design.¹⁹ Additionally, this was particularly of interest with the difference in stray field available to polarize nuclei with flow analyses for high-field systems with superconducting magnets and benchtop NMR systems with permanent magnets.³³ Therefore, activation of the same carboxylic acid **4** with PBSF (**6**) was performed under the same flow conditions (concentration, flow rate, *etc.*) but monitored via ^{19}F NMR at 471 MHz (Figure 8, see Supporting Information Section S2.d for a system setup). In effort to probe the question, the reaction initially was monitored under *on-line* continuous-flow conditions, but part way through the reaction course, the pump was turned off, and the monitoring continued under static conditions for the remainder of the time course.

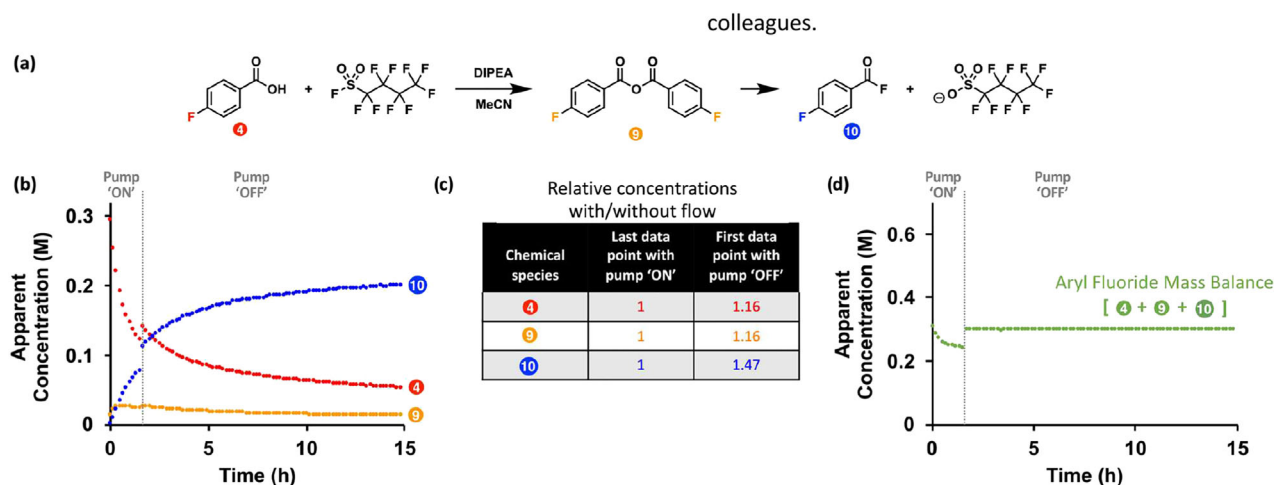


FIGURE 8 (a) Reaction scheme for the activation of **4** (0.30 M, $\delta_{\text{F}} -112.5$ ppm) with **6** (1.1 eq.) to form the corresponding acyl fluoride **10** ($\delta_{\text{F}} -101.3$ ppm) in MeCN with DIPEA (1.2 eq.). (b) Observed reaction trends resulting from tracking each ^{19}F resonance (471 MHz) of interest, with the pump turned 'off' part way through the reaction course. (c) Relative normalized comparisons of last point with pump 'on' and first point with pump 'off'. (d) Uncorrected mass balance analysis as result of tracking the sum of aryl fluoride components over time.

The same polarization phenomenon was observed under the same conditions but monitoring via high-field NMR. This was particularly evident by comparing the apparent concentrations of the last data point with the pump 'on' and the first data point with the pump 'off' for starting material **4**, intermediate **9** and product **10** (Figure 8). With all the final data points with the pump 'on' normalized, the integrations for resonance of both starting material **4** and intermediate **9** increased by 16%. While it is expected that integrations would increase with the flow halted (for reasons highlighted in previous discussion regarding T_1 and polarization), the integral values for all species were expected to increase by the same relative amount if the same relative polarization was achieved prior to spectral measurement. Instead, we observed a much larger (47%) increase in resonance integration for product **10**.

The difference in relative for the last data point with the pump 'on' and the first point with the pump 'off' can be rationalized based on the estimated T_1 values. The significantly large relative difference for the aryl fluoride resonance of product **10** suggested that an unequal proportion of spins remained unpolarized in continuous-flow conditions, compared with starting material **4** and intermediate **9** prior to acquiring the fluorine spectra. This result is consistent with the 'in-flow' effects of flow NMR, where the long estimated T_1 (14.7 s) for **10** suggests that a smaller proportion of spins may be polarized for a given flow rate relative to starting material **4** (estimated T_1 of 4.7 s). Then upon halting the reaction mixture in the instrument, all the spins existed in the external magnetic field such that over 99% polarization was achieved prior to spectral measurement, regardless of the specific resonance.

Additionally, through monitoring the aryl fluoride apparent mass balance for carboxylic acid starting material **4**, symmetric anhydride intermediate **9**, and acyl fluoride **10** for the same trial, interesting behaviour is observed (Figure 8d). During the first part of the reaction, when the system was monitored via *on-line* continuous-flow, one can observe similar downward trend to that observed in the *on-line* continuous-flow trial utilizing the benchtop NMR. Then once the pump is turned off the mass balance becomes, as expected, linear with a slope of zero. These data are therefore consistent with previous observations and further are consistent with inadequate polarization for the *on-line* continuous-flow conditions used, even when acquired with a different magnet geometry and high-field NMR spectrometer.

4 | CONCLUSION

With the increase in commercially available benchtop NMR instruments and associated flow systems, the potential for NMR to serve as a convenient process analytical technology is ever increasing. With such a system, a reaction can be easily monitored via *on-line* stopped-flow (flowing reaction solution to the NMR, stopping the solution, acquiring a spectrum, repeat) or *on-line* continuous-flow (acquire NMR spectrum as solution is flowing through NMR). As in the literature it has been reported on the substantial difference one may observe in reactions performed in a 5 mm NMR tube and those monitored by continuous-flow,¹³ we sought to compare *on-line* stopped-flow and continuous-flow sampling methods for NMR reaction monitoring.

Our work suggests that even in instances where the resulting reaction trends may agree between sampling techniques, there will always be an inherent SNR benefit to *on-line* stopped-flow analyses as maximum polarization of NMR active spins for a particular volume may be achieved, considering the data measured with the same acquisition parameters. This difference in SNR may be particularly of interest to benchtop NMR users with the sensitivity limitation inherent to benchtop instruments. The work presented on the homogeneous imination reaction particularly showcases the SNR differences as described. It should be noted that under *on-line* continuous-flow conditions, however, either a higher degree of data density could be collected, or data can be collected with more scans to improve SNR.

Furthermore, the work presented on the heterogeneous activation of a 4-fluorobenzoic acid (**4**) to the corresponding acyl fluoride (**10**) using PBSF (**6**) highlights where one can observe differences in reaction profiles between *on-line* stopped-flow and continuous-flow trials—when the T_1 of a resonance of interest is long. In this case, *on-line* continuous-flow conditions may not allow for appropriate polarization to accurately characterize a given profile. It is important to note that correction factors may be applied to compensate for ‘in-flow’ effects. However, under dynamic reaction conditions, a change in T_1 (due to change in concentration or solvent viscosity) or change in flow rate (due to change in reaction mixture viscosity) may make for challenging corrections. Additionally, our work highlights that this may not solely be a limitation of benchtop NMR systems, as the same observations resulted with the same reaction system monitored with a high-field NMR system.

In the interest of furthering benchtop NMR as an accessible reaction monitoring tool for non-NMR specialists, *on-line* stopped-flow analyses allow under quantitative conditions without correction factors for T_1 and with the convenience of using a flow system. While reaction monitoring under *on-line* continuous-flow conditions may be the method of choice for a faster reactions due to higher data density, *on-line* stopped-flow analyses can enhance the ease of ensuring the quantitative nature of the benchtop NMR reaction data.

ACKNOWLEDGEMENTS

The authors would like to thank Jiayu Zhang (UBC) with assistance with Python coding. Financial support for this work was provided by Genentech Inc., The University of British Columbia, the Canada Foundation for Innovation (CFI) (CFI-35883) and the Natural Sciences and Engineering Research Council of Canada


(NSERC) (RGPIN-2021-03168, Discovery Accelerator Supplement RGPAS-2021-00016).

PEER REVIEW

The peer review history for this article is available at <https://www.webofscience.com/api/gateway/wos/peer-review/10.1002/mrc.5395>.

ORCID

Tristan Maschmeyer  <https://orcid.org/0000-0002-9472-6747>

José G. Napolitano  <https://orcid.org/0000-0003-1250-2262>

Jason E. Hein  <https://orcid.org/0000-0002-4345-3005>

REFERENCES

- [1] F. Malz, H. Jancke, *J. Pharm. Biomed. Anal.* **2005**, *38*, 813.
- [2] E. Danieli, J. Perlo, A. L. L. Duchateau, G. K. M. Verzijl, V. M. Litvinov, B. Blümich, F. Casanova, *ChemPhysChem* **2014**, *15*, 3060.
- [3] W. G. Lee, M. T. Zell, T. Ouchi, M. J. Milton, *Magn. Reson. Chem.* **2020**, *58*, 1193.
- [4] S. D. Riegel, G. M. Leskowitz, *TrAC Trends Anal. Chem.* **2016**, *83*, 27.
- [5] P. M. Richardson, A. J. Parrott, O. Semenova, A. Nordon, S. B. Duckett, M. E. Halse, *Analyst* **2018**, *143*, 3442.
- [6] H. Chae, S. Min, H. J. Jeong, S. K. Namgoong, S. Oh, K. Kim, K. Jeong, *Anal. Chem.* **2020**, *92*, 10902.
- [7] T. H. Rehm, C. Hofmann, D. Reinhard, H.-J. Kost, P. Löb, M. Besold, K. Welzel, J. Barten, A. Didenko, D. V. Sevenard, B. Lix, A. R. Hillson, S. D. Riegel, *React. Chem. Eng.* **2017**, *2*, 315.
- [8] T. Maschmeyer, P. L. Prieto, S. Grunert, J. E. Hein, *Magn. Reson. Chem.* **2020**, *58*, 1234.
- [9] T. Maschmeyer, L. P. E. Yunker, J. E. Hein, *React. Chem. Eng.* **2022**, *7*, 1061.
- [10] L. Tadiello, H.-J. Drexler, T. Beweries, *Organometallics* **2022**, *41*, 2833.
- [11] K. Krishnamurthy, *Magn. Reson. Chem.* **2013**, *51*, 821.
- [12] K. Krishnamurthy, *Magn. Reson. Chem.* **2021**, *59*, 757.
- [13] D. A. Foley, A. L. Dunn, M. T. Zell, *Magn. Reson. Chem.* **2016**, *54*, 451.
- [14] A. Nordon, C. A. McGill, D. Littlejohn, *Analyst* **2001**, *126*, 260.
- [15] A. Nordon, A. Diez-Lazaro, C. W. L. Wong, C. A. McGill, D. Littlejohn, M. Weerasinghe, D. A. Mammann, M. L. Hitchman, J. Wilkie, *Analyst* **2008**, *133*, 339.
- [16] F. Dalitz, L. Kreckel, M. Maiwald, G. Guthausen, *Appl. Magn. Reson.* **2014**, *45*, 411.
- [17] F. Dalitz, M. Maiwald, G. Guthausen, *Chem. Eng. Sci.* **2012**, *75*, 318.
- [18] A. Saib, A. Bara-Estaún, O. J. Harper, D. B. G. Berry, I. A. Thomlinson, R. Broomfield-Tagg, J. P. Lowe, C. L. Lyall, U. Hintermair, *React. Chem. Eng.* **2021**, *6*, 1548.
- [19] A. M. R. Hall, J. C. Chouler, A. Codina, P. T. Gierth, J. P. Lowe, U. Hintermair, *Cat. Sci. Technol.* **2016**, *6*, 8406.
- [20] R. Neudert, E. Ströfer, W. Bremser, *Magn. Reson. Chem.* **1986**, *24*, 1089.

- [21] A. García-Domínguez, T. H. West, J. J. Primožic, K. M. Grant, C. P. Johnston, G. C. Cumming, A. G. Leach, G. C. Lloyd-Jones, *J. Am. Chem. Soc.* **2020**, *142*, 14649.
- [22] C. P. Johnston, T. H. West, R. E. Dooley, M. Reid, A. B. Jones, E. J. King, A. G. Leach, G. C. Lloyd-Jones, *J. Am. Chem. Soc.* **2018**, *140*, 11112.
- [23] R. Wei, A. M. R. Hall, R. Behrens, M. S. Pritchard, E. J. King, G. C. Lloyd-Jones, *Eur. J. Org. Chem.* **2021**, *2021*, 2331.
- [24] R. L. Vold, J. S. Waugh, M. P. Klein, D. E. Phelps, *J. Chem. Phys.* **1968**, *48*, 2831.
- [25] R. Freeman, H. D. W. Hill, *J. Chem. Phys.* **1969**, *51*, 3140.
- [26] R. Wei, C. L. Dickson, D. Uhrin, G. C. Lloyd-Jones, *J. Org. Chem.* **2021**, *86*, 9023.
- [27] A. Bara-Estaún, M. C. Harder, C. L. Lyall, J. P. Lowe, E. Suturina, U. Hintermair, *Chem. A Eur. J.* **2023**, *29*, e202300215.
- [28] S. K. Bharti, N. Sinha, B. S. Joshi, S. K. Mandal, R. Roy, C. L. Khetrpal, *Metabolomics* **2008**, *4*, 367.
- [29] B. Bennua-Skalmowski, H. Vorbrüggen, *Tetrahedron Lett.* **1995**, *36*, 2611.
- [30] P. J. Foth, T. C. Malig, H. Yu, T. G. Bolduc, J. E. Hein, G. M. Sammis, *Org. Lett.* **2020**, *22*, 6682.
- [31] R. W. Mitchell, M. Eisner, *J. Chem. Phys.* **1961**, *34*, 651.
- [32] K. Hatada, T. Kitayama, Y. Terawaki, Y. Tanaka, H. Sato, *Polym. Bull.* **1980**, *2*, 791.
- [33] N. Zientek, C. Laurain, K. Meyer, M. Kraume, G. Guthausen, M. Maiwald, *J. Magn. Reson.* **2014**, *249*, 53.

SUPPORTING INFORMATION

Additional supporting information can be found online in the Supporting Information section at the end of this article.

How to cite this article: T. Maschmeyer, D. J. Russell, J. G. Napolitano, J. E. Hein, *Magn Reson Chem* **2023**, *1*, <https://doi.org/10.1002/mrc.5395>